A VARIATIONAL FINITE LAYER TECHNIQUE FOR THE INVESTIGATION OF REINFORCEMENT PATCH CORNERS

Hubertus M. Wigger*, Wilfried Becker* [Wigger]: wigger@mechanik.tu-darmstadt.de
***Technische Universität Darmstadt, Fachbereich Maschinenbau,**
Fachgebiet Strukturmechanik

Keywords: Laminates, Interlaminar Stress, Closed-Form Analysis, Variational Finite Layer Technique

Abstract

A closed-form approach for the calculation of the interlaminar stress concentrations in the surroundings of rectangular reinforcement patch corners of thermally loaded composite cross-ply laminates is presented. The interlaminar stresses are obtained by the application of a perturbing stress field superposed to the results of the classical laminate plate theory. The perturbing stress field comprises stress functions which are separable in regard to the dependency on transverse and in-plane coordinates. Based on continuity considerations the transverse part is assumed a priori to be known. The general form of the in-plane coordinate dependent part is determined with the help of the principle of minimum complementary potential energy. For the particular form boundary conditions are applied using an expanded Ritz-approach with Lagrange multipliers. The method is in good agreement with results from a comparative finite element analysis, is easily applicable and requires very low computational effort.

1 Introduction

Laminate patches are commonly used in lightweight constructions to reinforce laminate plate locations which have to endure a higher load than the remaining base plate structure. At the edges and particularly at the corners of such reinforcement patches, see Fig. 1, stress concentrations occur which include interlaminar stresses evoked by the discontinuous change of the corresponding in-plane stiffness. These interlaminar stresses are not properly accounted for by the classical laminate plate theory (CLPT) which is the usual means to assess the mechanical behavior of layered plates [1].

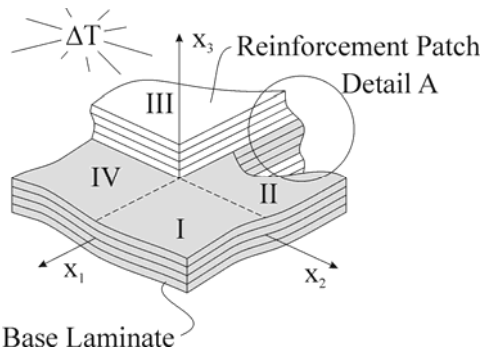

Fig. 1. General structural setup of a reinforcement patch corner

Thus, this structural configuration belongs to the same class of problems in elasto-mechanics like the free-edge effect, see the literature surveys [2], [3] and [4], or the free-corner effect, which has been investigated e.g. by Becker et al. [5] or Mittelstedt and Becker [6]. But unlike the latter structural setup the present problem contains a base laminate which complicates the investigation since it can not be addressed with the instruments used to analyze the free-edge effect. Here the present approach makes use of the stress function representation as it has been suggested by Bhat and Lagace [7] for dealing with material discontinuities of laminate plies. For laminates discretized in the transverse direction with only one layer per ply the presented approach has already been applied successfully by Wigger and Becker [8].

2 Analysis Approach

2.1 Stress Fields

Under consideration for analysis is a cross-ply base laminate which is reinforced symmetrically in the transverse direction by cross-ply laminate patches. The laminates' lay-ups are assumed to be symmetric and the corner of the laminate patches regarded is rectangular. The structure is subjected to an assumed constant temperature change ΔT, see Fig. 1 where the position of the global coordinate system of the whole structure is also depicted. Due to the symmetry of the laminate only the upper half consisting of n plies is examined, see Fig. 2.

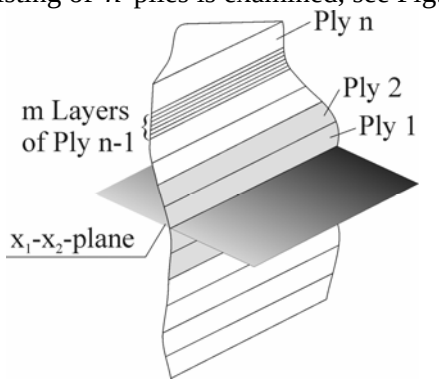

Fig. 2. Detail A of Fig.1 with ply numbering convention

The n plies are divided each into m mathematical layers and each layer has its own local coordinate system with a local $x_1^{(i)}$ - $x_2^{(i)}$ -plane as the mid-plane of the layer and the $x_3^{(i)}$ -axis running along the global x_3 -axis, see Fig. 3.

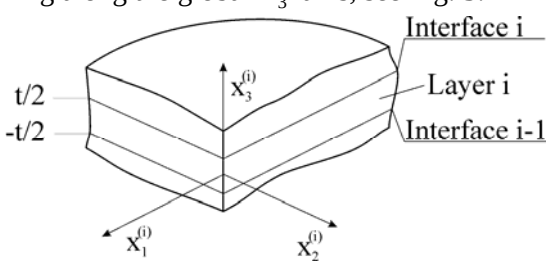

Fig. 3. Nomenclature of layer

The structure around the x_3 -axis is partitioned into four domains which correspond to the projections of the four quadrants of the x_1 - x_2 -plane. So the base laminate lies in quadrants I, II and IV while the reinforcement corner domain is located in quadrant III, see Fig. 1. The domain Ω^{III} differs from the three others only by the reinforcement laminates' plies and their boundary conditions which are accounted for at a later step of the analysis formulation. Therefore, the approach is presented first in a general form without referring to one special domain.

In regions where the assumptions of the plane stress situation are valid the classical laminate plate theory (CLPT) holds. At locations like e.g. edges or ply drop-offs this is no longer true since the geometrical and/or material discontinuity evolves a three-dimensional stress state from the plane stress situation so the in-plane stresses from the CLPT can fulfill the respective boundary or transition conditions only in an integral sense. Hence it is appropriate to describe the stress state at such locations as a superposition of the in-plane stresses from the CLPT and a perturbing stress field (PSF) which in conjunction with the CLPT-stresses satisfies the conditions of the respective discontinuity on a ply-by-ply basis.

Hence, the in-plane stresses in an individual ply (i) can be written as

$$\sigma_{11}^{(i)} = \sigma_{11}^{(i)CLPT} + \sigma_{11}^{(i)PSF}, \tag{1}$$

$$\sigma_{22}^{(i)} = \sigma_{22}^{(i)CLPT} + \sigma_{22}^{(i)PSF}, \tag{2}$$

$$\sigma_{12}^{(i)} = \sigma_{12}^{(i)CLPT} + \sigma_{12}^{(i)PSF}. \tag{3}$$

The three-dimensional equilibrium conditions with vanishing volume forces for the (i) -th layer read

$$\frac{\partial \sigma_{11}^{(i)}}{\partial x_1} + \frac{\partial \sigma_{12}^{(i)}}{\partial x_2} + \frac{\partial \sigma_{13}^{(i)}}{\partial x_3} = 0, \tag{4}$$

$$\frac{\partial \sigma_{12}^{(i)}}{\partial x_1} + \frac{\partial \sigma_{22}^{(i)}}{\partial x_2} + \frac{\partial \sigma_{23}^{(i)}}{\partial x_3} = 0, \tag{5}$$

$$\frac{\partial \sigma_{13}^{(i)}}{\partial x_1} + \frac{\partial \sigma_{23}^{(i)}}{\partial x_2} + \frac{\partial \sigma_{33}^{(i)}}{\partial x_3} = 0. \tag{6}$$

For a thermal loading situation in each of the domains I to IV the in-plane stresses from CLPT are constant in the respective layer and thus only stress components from the PSF appear in Eqs. (4)-(6). Furthermore, considering just symmetric cross-ply laminates the stress component $\sigma_{12}^{(i)}$ vanishes, so the interlaminar stresses for a layer can be obtained as

$$\sigma_{13}^{(i)PSF}(\tfrac{t}{2})-\sigma_{13}^{(i)PSF}(x_3^{(i)})=-\int_{x_3^{(i)}}^{\frac{t}{2}}\frac{\partial\sigma_{11}^{(i)PSF}}{\partial x_1}d\hat{x}_3^{(i)}, \tag{7}$$

$$\sigma_{23}^{(i)PSF}(\tfrac{t}{2})-\sigma_{23}^{(i)PSF}(x_3^{(i)})=-\int_{x_3^{(i)}}^{\frac{t}{2}}\frac{\partial\sigma_{22}^{(i)PSF}}{\partial x_2}d\hat{x}_3^{(i)}, \tag{8}$$

$$\sigma_{33}^{(i)PSF}(\tfrac{t}{2})-\sigma_{33}^{(i)PSF}(x_3^{(i)})=-\int_{x_3^{(i)}}^{\frac{t}{2}}\left(\frac{\partial\sigma_{13}^{(i)PSF}}{\partial x_1}+\frac{\partial\sigma_{23}^{(i)PSF}}{\partial x_2}\right)d\hat{x}_3^{(i)} \tag{9}$$

where an additional assumption is that each layer is of thickness t. Now the conditions of continuity of the interlaminar stress components at the interfaces of the mathematical layers as well as the traction free upper surface have to be taken into account. In view of these conditions the stress components of the PSF are assumed to be separable in product form, where one factor comprises the functional dependence of the stress functions on the in-plane coordinates x_1 and x_2 and the other factor is a polynomial which interpolates these in-plane dependent functions through the thickness $x_3^{(i)}$ within each layer (i). Thus, for the in-plane stress components the following representation is chosen

$$\begin{aligned}\sigma_{11}^{PSF(i)} &= D_1^{(i-1)}(x_1)F^{(i-1)}(x_3^{(i)})\\ &\quad - D_1^{(i)}(x_1)F^{(i)}(x_3^{(i)}),\end{aligned} \tag{10}$$

$$\begin{aligned}\sigma_{22}^{PSF(i)} &= D_2^{(i-1)}(x_2)F^{(i-1)}(x_3^{(i)})\\ &\quad - D_2^{(i)}(x_2)F^{(i)}(x_3^{(i)}),\end{aligned} \tag{11}$$

where the unknown in-plane functions $D_1^{(i-1)}$, $D_2^{(i-1)}$ and $D_1^{(i)}$, $D_2^{(i)}$ are located at the bottom and top interface of the (i)-th layer, respectively. The interlaminar stresses are obtained with the help of Eqs. (7) - (9) as

$$\begin{aligned}\sigma_{13}^{(i)PSF}(x_3^{(i)}) &= D_{1,1}^{(i-1)}(x_1)\int_{x_3^{(i)}}^{\frac{t}{2}}F^{(i-1)}d\hat{x}_3^{(i)}\\ &\quad - D_{1,1}^{(i)}(x_1)\int_{x_3^{(i)}}^{\frac{t}{2}}F^{(i)}d\hat{x}_3^{(i)}+\sigma_{13}^{(i)PSF}(\tfrac{t}{2}),\end{aligned} \tag{12}$$

$$\begin{aligned}\sigma_{23}^{(i)PSF}(x_3^{(i)}) &= D_{2,2}^{(i-1)}(x_2)\int_{x_3^{(i)}}^{\frac{t}{2}}F^{(i-1)}d\hat{x}_3^{(i)}\\ &\quad - D_{2,2}^{(i)}(x_2)\int_{x_3^{(i)}}^{\frac{t}{2}}F^{(i)}d\hat{x}_3^{(i)}+\sigma_{23}^{(i)PSF}(\tfrac{t}{2}),\end{aligned} \tag{13}$$

$$\begin{aligned}\sigma_{33}^{(i)PSF}(x_3^{(i)}) &= \left(D_{1,11}^{(i-1)}(x_1)+D_{2,22}^{(i-1)}(x_2)\right)\int_{x_3^{(i)}}^{\frac{t}{2}}\left(\int_{x_3^{(i)}}^{\frac{t}{2}}F^{(i-1)}d\hat{x}_3^{(i)}\right)d\hat{x}_3^{(i)}\\ &\quad -\left(D_{1,11}^{(i)}(x_1)+D_{2,22}^{(i)}(x_2)\right)\int_{x_3^{(i)}}^{\frac{t}{2}}\left(\int_{x_3^{(i)}}^{\frac{t}{2}}F^{(i)}d\hat{x}_3^{(i)}\right)d\hat{x}_3^{(i)}\\ &\quad +\int_{x_3^{(i)}}^{\frac{t}{2}}\left(\frac{\partial\sigma_{13}^{PSF(i)}(\frac{t}{2})}{\partial x_1}+\frac{\partial\sigma_{23}^{PSF(i)}(\frac{t}{2})}{\partial x_2}\right)d\hat{x}_3^{(i)}\\ &\quad +\sigma_{33}^{(i)PSF}(\tfrac{t}{2}).\end{aligned} \tag{14}$$

Here, $(...)_{,1}$, $(...)_{,11}$ and $(...)_{,2}$, $(...)_{,22}$ mean first and second derivatives with respect to x_1 and x_2, respectively.

As the simplest possibility the polynomial interpolation functions $F^{(i-1)}$ and $F^{(i)}$ are chosen to be

$$F^{(i-1)}=\frac{1}{t}, \tag{15}$$

$$F^{(i)}=\frac{1}{t}, \tag{16}$$

with t as the individual thickness of each layer. The integration of the interpolating functions of the interlaminar shear stresses with respect to the transversal coordinate $x_3^{(i)}$ is performed with the assumption that the influence of the first derivatives of the in-plane functions $D_1^{(i)}$, $D_2^{(i)}$ vanishes towards the next adjacent interface. Accordingly, the interpolation functions for the interlaminar stresses are

$$\int_{x_3^{(i)}}^{\frac{t}{2}}F^{(i-1)}d\hat{x}_3^{(i)}=\frac{1}{2}-\frac{x_3^{(i)}}{t}, \tag{17}$$

$$1-\int_{x_3^{(i)}}^{\frac{t}{2}} F^{(i)} d\hat{x}_3^{(i)} = \frac{1}{2}+\frac{x_3^{(i)}}{t}, \tag{18}$$

$$\int_{x_3^{(i)}}^{\frac{t}{2}} \left(\int_{x_3^{(i)}}^{\frac{t}{2}} F^{(i-1)} d\hat{x}_3^{(i)} \right) d\hat{x}_3^{(i)} = \frac{t}{2}\left[\frac{x_3^{(i)}}{t}-\frac{1}{2}\right]^2, \tag{19}$$

$$\int_{x_3^{(i)}}^{\frac{t}{2}} \left(1-\int_{x_3^{(i)}}^{\frac{t}{2}} F^{(i)} d\hat{x}_3^{(i)} \right) d\hat{x}_3^{(i)} = -\frac{t}{2}\left[\frac{x_3^{(i)}}{t}+\frac{1}{2}\right]^2+\frac{t}{2} \tag{20}$$

Now, the integration constants $\sigma_{13}^{(i)PSF}(\frac{t}{2})$, $\sigma_{23}^{(i)PSF}(\frac{t}{2})$ and $\sigma_{33}^{(i)PSF}(\frac{t}{2})$ in Eqs. (12) to (14) can be evaluated as

$$\sigma_{13}^{(i)PSF}(\tfrac{t}{2}) = D_{1,1}^{(i)}(x_1), \tag{21}$$

$$\sigma_{23}^{(i)PSF}(\tfrac{t}{2}) = D_{2,2}^{(i)}(x_2), \tag{22}$$

$$\begin{aligned}\sigma_{33}^{(i)PSF}(\tfrac{t}{2}) = &-D_{l,ll}^{(i)}(x_l)\frac{t}{2} \\ &+\sum_{k=i+1}^{m(p(i))} D_{l,ll}^{(k)}(x_l)\,t \\ &+\sum_{h=p(i)+1}^{n-1}\sum_{k=0}^{m(h)} D_{l,ll}^{(k)}(x_l)\,t \\ &+\sum_{k=0}^{m(n)-1} D_{l,ll}^{(k)}(x_l)\,t.\end{aligned} \tag{23}$$

The continuity condition and the condition that the upper surface of the laminate is traction free have been taken into account for the integration constants of the interpolating function of the interlaminar normal stress $\sigma_{33}^{(i)PSF}$.

For the in-plane functions there has also to be kept in mind that the traction free upper surface means that the second derivatives of the in-plane functions vanish at the $(n \cdot m)$ -th interface. Furthermore, due to symmetric lay-ups there are no interlaminar shear stresses at the mid-plane and hence the first derivatives of the in-plane functions are identical zero at the (0) -th interface. As a consequence from both preceding considerations no in-plane functions exist at those interfaces because otherwise the CLPT-results far away from the perturbation location would be altered.

2.2 General Form of PSF-Stresses

In order to determine the in-plane functions $D_1^{(i)}$ and $D_2^{(i)}$ the principle of minimum total complementary potential energy $\tilde{\Pi}$ is applied. For the case of the regarded upper half of the laminate with linear-elastic material properties under thermal loading the total complementary potential energy $\tilde{\Pi}$ reads

$$\begin{aligned}\tilde{\Pi} = &\frac{1}{2}\sum_{p=1}^{n}\sum_{i(p)=1}^{m(p)}\iiint_{V^{(i)}} \sigma^{(i)T}\mathbf{S}^{(i)}\sigma^{(i)}\,dV^{(i)} \\ &+\sum_{p=1}^{n}\sum_{i(p)=1}^{m(p)}\iiint_{V^{(i)}} \sigma^{(i)T}\alpha_{th}^{(i)}\Delta T\,dV^{(i)}\end{aligned} \tag{24}$$

Herein, $\sigma^{(i)}$ denotes the array of the components of Cauchy's stress tensor compiled as

$$\sigma^{(i)} = \left(\sigma_{11}^{(i)}\ \sigma_{22}^{(i)}\ \sigma_{33}^{(i)}\ \sigma_{23}^{(i)}\ \sigma_{13}^{(i)}\ \sigma_{12}^{(i)}\right)^T, \tag{25}$$

$\mathbf{S}^{(i)}$ is the compliance matrix of the (i) -th linear elastic layer, for which orthotropic material behavior is assumed

$$\mathbf{S}^{(i)} = \begin{bmatrix} S_{11}^{(i)} & S_{12}^{(i)} & S_{13}^{(i)} & 0 & 0 & 0 \\ S_{12}^{(i)} & S_{22}^{(i)} & S_{23}^{(i)} & 0 & 0 & 0 \\ S_{13}^{(i)} & S_{23}^{(i)} & S_{33}^{(i)} & 0 & 0 & 0 \\ 0 & 0 & 0 & S_{44}^{(i)} & 0 & 0 \\ 0 & 0 & 0 & 0 & S_{55}^{(i)} & 0 \\ 0 & 0 & 0 & 0 & 0 & S_{66}^{(i)} \end{bmatrix}, \tag{26}$$

$\alpha_{th}^{(i)}$ are the compiled coefficients of thermal expansion

$$\alpha_{th}^{(i)} = \left(\alpha_{11th}^{(i)}\ \alpha_{22th}^{(i)}\ \alpha_{33th}^{(i)}\ 0\ 0\ 0\right)^T \tag{27}$$

and ΔT is the temperature change from stress free conditions in the layer volume $V^{(i)}$.

If now the superposition of the CLPT and the PSF stresses is regarded and Eq. (24) is expanded three terms are obtained. The first term contains the complementary potential energy of the CLPT and is consequently of no interest. The second term composes of stresses from the PSF and the

CLPT strains array ε^{CLPT}. Since the components of this strains array are constant through the thickness of the laminate and the plies are assumed to be of identical thickness, integration with respect to the transversal direction yields no contributions to the total complementary potential energy. This leaves only the third term

$$\tilde{\Pi}_3 = \frac{1}{2}\sum_{p=1}^{n}\sum_{i(p)=1}^{m(p)}\iiint_{V^{(i)}}(\sigma^{(i)PSF})^T\mathbf{S}^{(i)}\sigma^{(i)PSF}dV^{(i)} \tag{28}$$

For the minimization of the total complementary potential energy the first variation $\delta\tilde{\Pi}$ of $\tilde{\Pi}$ or equivalently $\delta\tilde{\Pi}_3$ has to vanish

$$\delta\tilde{\Pi}_3 \overset{!}{=} 0. \tag{29}$$

Defining the function G as follows

$$G = \frac{1}{2}\sum_{p=1}^{n}\sum_{i(p)=1}^{m}\int_{-\frac{t}{2}}^{\frac{t}{2}}(\sigma^{(i)PSF})^T\mathbf{S}^{(i)}\sigma^{(i)PSF}d\hat{x}_3^{(i)} \tag{30}$$

and performing the integration with respect to the transversal coordinates $x_3^{(i)}$, G depends only on the unknown functions $D_1^{(i)}(x_1)$ and $D_2^{(i)}(x_2)$. Thus, $\tilde{\Pi}_3$ has a stationary value if the variations corresponding Euler-Lagrange equations

$$\frac{\partial G}{\partial D_1^{(i)}} - \frac{d}{dx_1}\left(\frac{\partial G}{\partial D_{1,1}^{(i)}}\right) + \frac{d^2}{dx_1^2}\left(\frac{\partial G}{\partial D_{1,11}^{(i)}}\right) = 0, \tag{31}$$

$$\frac{\partial G}{\partial D_2^{(i)}} - \frac{d}{dx_2}\left(\frac{\partial G}{\partial D_{2,2}^{(i)}}\right) + \frac{d^2}{dx_2^2}\left(\frac{\partial G}{\partial D_{2,22}^{(i)}}\right) = 0, \tag{32}$$

are satisfied, with $(i(p) = 0,1,\ldots,m)$ and $(p = 1,2,\ldots,n)$. A system of coupled ordinary linear fourth-order Euler-Lagrange differential equations is obtained from this variation as

$$\begin{aligned} 0 = {} & \mathbf{K}_{14}^{(i)}\mathbf{D}_{1,1111} + \mathbf{K}_{12}^{(i)}\mathbf{D}_{1,11} + \mathbf{K}_{10}^{(i)}\mathbf{D}_1 \\ & + \mathbf{H}_{12}^{(i)}\mathbf{D}_{2,22} + \mathbf{H}_{10}^{(i)}\mathbf{D}_2 \end{aligned} \tag{33}$$

$$\begin{aligned} 0 = {} & \mathbf{H}_{24}^{(i)}\mathbf{D}_{2,2222} + \mathbf{H}_{22}^{(i)}\mathbf{D}_{2,22} + \mathbf{H}_{20}^{(i)}\mathbf{D}_2 \\ & + \mathbf{K}_{22}^{(i)}\mathbf{D}_{1,11} + \mathbf{K}_{20}^{(i)}\mathbf{D}_1^{(i)} \end{aligned} \tag{34}$$

Herein, the vectors $\mathbf{D}_1$, $\mathbf{D}_2$ and their respective derivatives are compiled of the stress representatives $D_1^{(i)}$ and $D_2^{(i)}$ and their derivatives. The coefficients of the row vectors $\mathbf{K}_{14}^{(i)}$, $\mathbf{K}_{12}^{(i)}$, $\mathbf{K}_{10}^{(i)}$, $\mathbf{K}_{22}^{(i)}$, $\mathbf{K}_{20}^{(i)}$ and $\mathbf{H}_{12}^{(i)}$, $\mathbf{H}_{10}^{(i)}$, $\mathbf{H}_{24}^{(i)}$, $\mathbf{H}_{22}^{(i)}$, $\mathbf{H}_{20}^{(i)}$ are given in detail in reference [8].

The order of this set of differential equations can be reduced by rearranging the equations. Then the obtained set of homogeneous differential equations can be transformed into a related eigenvalue problem which has a solution for the in-plane functions of the following kind

$$D_1^{(i)} = \sum_{j=1}^{2(n\cdot m-1)} c_{1j}\phi_j^{(i)}e^{\lambda_j x_1} \tag{35}$$

$$D_2^{(i)} = \sum_{j=1}^{2(n\cdot m-1)} c_{2j}\psi_j^{(i)}e^{\mu_j x_2} \tag{36}$$

with λ_j and μ_j as the eigenvalues and $\phi_j^{(i)}$ and $\psi_j^{(i)}$ as the eigenvectors. The only unknown quantities in the foregoing expressions are the constants c_{1j} and c_{2j}. These have now to be determined by the use of the boundary and transition conditions at the laminate reinforcement corner.

2.3 Particular Form of PSF-Stresses

The constants c_{1j} and c_{2j} are obtained by utilizing the conditions which have to be satisfied at the common boundary of domain Ω^{III} and domain Ω^{II} as well as at the boundary shared by domain Ω^{III} and domain Ω^{IV}. At the stress free edges of the reinforcement patch the PSF-stresses in the layers have to comply with the following boundary conditions

$$B_1^{(i)} = \sigma_{11}^{(i)III}\Big|_{x_1=0} = 0, \tag{37}$$

$$B_2^{(i)} = \sigma_{13}^{(i)III}\Big|_{x_1=0,\,x_3^{(i)}=-\frac{t}{2}} = 0, \tag{38}$$

$$B_3^{(i)} = \sigma_{22}^{(i)III}\Big|_{x_2=0} = 0, \tag{39}$$

$$B_4^{(i)} = \sigma_{23}^{(i)III}\Big|_{x_2=0,x_3^{(i)}=-\frac{t}{2}} = 0, \tag{40}$$

where i is a layer of a ply p for which $n_{IV} < p(i) \le n_{III}$ holds, n_{IV} as the number of plies in the base laminate and n_{III} as the number of plies in the reinforced domain of the base laminate. For the PSF-stresses in the continuous layers of the base laminate only the transition conditions are known, not the particular matching stress values at the domain boundaries, so this reads

$$T_1^{(i)} = \left(\sigma_{11}^{(i)III} - \sigma_{11}^{(i)IV}\right)\Big|_{x_1=0} = 0, \tag{41}$$

$$T_2^{(i)} = \left(\sigma_{13}^{(i)III} - \sigma_{13}^{(i)IV}\right)\Big|_{x_1=0,x_3^{(i)}=-\frac{t}{2}} = 0, \tag{42}$$

$$T_3^{(i)} = \left(\sigma_{22}^{(i)III} - \sigma_{22}^{(i)IV}\right)\Big|_{x_2=0} = 0, \tag{43}$$

$$T_4^{(i)} = \left(\sigma_{23}^{(i)III} - \sigma_{23}^{(i)IV}\right)\Big|_{x_2=0,x_3^{(i)}=-\frac{t}{2}} = 0 \tag{44}$$

with $1 < p(i) \le n_{IV}$. In this way additional unknowns are introduced to the problem which thus can not be solved algebraically but has to be approached by a minimization technique. Therefore, an expanded Ritz method is used where the afore formulated boundary and transition conditions are incorporated with the help of Lagrange multipliers. The function to be minimized reads

$$\begin{aligned}\Pi_{Ritz} &= \tilde{\Pi}_3^{III} \\ &+ \tilde{\Pi}_3^{IV} \\ &+ \sum_{p=1}^{n_{IV}} \sum_{i(p)=1}^{m(p)} \alpha_1^{(i)} T_1^{(i)} + \sum_{p=1}^{n_{IV}} \sum_{i(p)=1}^{m(p)} \alpha_2^{(i)} T_2^{(i)} \\ &+ \sum_{p=n_{IV}}^{n_{III}} \sum_{i(p)=1}^{m(p)} \alpha_3^{(i)} B_1^{(i)} + \sum_{p=n_{IV}}^{n_{III}} \sum_{i(p)=1}^{m(p)} \alpha_4^{(i)} B_2^{(i)} \\ &+ \sum_{p=1}^{n_{IV}} \sum_{i(p)=1}^{m(p)} \beta_1^{(i)} T_3^{(i)} + \sum_{p=1}^{n_{IV}} \sum_{i(p)=1}^{m(p)} \beta_2^{(i)} T_4^{(i)} \\ &+ \sum_{p=n_{IV}}^{n_{III}} \sum_{i(p)=1}^{m(p)} \beta_3^{(i)} B_3^{(i)} + \sum_{p=n_{IV}}^{n_{III}} \sum_{i(p)=1}^{m(p)} \beta_4^{(i)} B_4^{(i)}\end{aligned} \tag{45}$$

where the first summand accounts for the complementary potential in domain Ω^{III} . The complementary potential of the base laminate is represented by the second summand comprising domain Ω^{IV} . Only one domain of the base laminate is used since domains Ω^{II} and Ω^{IV} are equivalent in their contribution to the complementary potential and domain Ω^{I} has no effect on this complementary potential.

The constraints from the boundary and transition conditions are incorporated into the formulation with Lagrange multipliers $\alpha_1^{(i)}$ to $\alpha_4^{(i)}$ imposed at the common boundary of domains Ω^{III} and Ω^{IV} and the multipliers $\beta_1^{(i)}$ to $\beta_4^{(i)}$ in effect at the boundary where domains Ω^{III} and Ω^{II} meet.

Then the minimum of Eq. (45) with respect to the unknown constants c_{1j}^{III} and c_{2j}^{III} of domain Ω^{III} and the unknown constants c_{1j}^{IV} and c_{2j}^{IV} of domain Ω^{IV} as well as the Lagrange multipliers is searched for by demanding

$$\frac{\partial \Pi_{Ritz}}{\partial c_{1j}^{III}} = 0 \tag{46}$$

$$\frac{\partial \Pi_{Ritz}}{\partial c_{2j}^{III}} = 0 \tag{47}$$

$$\frac{\partial \Pi_{Ritz}}{\partial c_{1j}^{IV}} = 0 \tag{48}$$

$$\frac{\partial \Pi_{Ritz}}{\partial c_{2j}^{IV}} = 0 \tag{49}$$

$$\frac{\partial \Pi_{Ritz}}{\partial \alpha_k^{(i)}} = 0 \tag{50}$$

$$\frac{\partial \Pi_{Ritz}}{\partial \beta_k^{(i)}} = 0 \tag{51}$$

With $(i(p) = 1,2,...,m)$, $(p = 1,2,...,n)$ $(j = 1,2,...,2(n \cdot m - 1))$ and $(k = 1,2,...,4)$. This results in an inhomogeneous system of linear equations which is solved for the constants c_{1j} and c_{2j} and the Lagrange multipliers, for details see reference [8]. Eventually the determined constants are used in Eqs (35) and (36) to obtain the PSF which in turn is superposed with the results of the CLPT.

3 Results and Discussion

3.1 Structural Configuration and Comparative Results for Validation

As an example a $[0^\circ/90^\circ]_S$ cross-ply lay-up is provided for base and reinforcement laminate, respectively, so the structure possesses transversal symmetry. Each ply within the structure is assumed to have an individual thickness of 0.25 mm which leads to a total base laminate thickness of $d = 1.0$ mm and a total reinforced laminate thickness of 3.0 mm. The employed material is the standard carbon fiber-reinforced plastic (CFRP) T800/Epoxy. A uniform temperature rise of $\Delta T = 100$ K is assumed as loading condition.
A comparative finite element analysis (FEA) has been performed in order to validate the obtained results from the closed-form approach. The standard commercial finite element code ABAQUS® has been employed and the applied element type is a displacement based isoparametric 8-noded volume element with three translational degrees of freedom per node. The discretization of the structure with finite elements resulted in a model with approx. 740,000 degrees of freedom. The geometry of the finite element model is depicted in Fig. 4. The meshing structure of the shown model is a similar but much coarser finite element representation than the actually used finite element mesh.

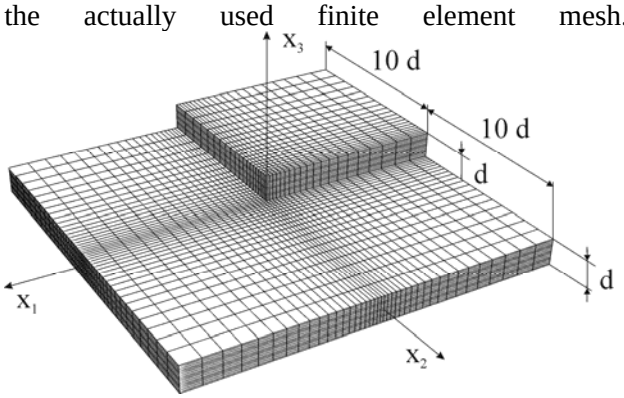

Fig. 4. Finite element discretization of the structural setup

The actual finite element representation possesses a more significant refinement towards the corner of the reinforcement patch and in the vicinity of the interfaces between the laminate plies. The interfaces of adjacent laminate plies receive the most attention since they are prominent spots of failure. But due to the inherent singular character of the stress field directly in these locations the results are computed at a small distance away.

3.2 Convergence Study

First, the present approach is investigated in regard to its behaviour with varying numbers of layers used for the discretization of the plies. The results for this investigation are attained at $x_3 = 0.375$ mm, the midplane of the second ply. As can be seen in Fig. 5 and 7 the results with a discretization of only one layer per ply resemble the overall qualitative behaviour of the interlaminar shear stress well. As expected, the results become better and converge if more layers are used.

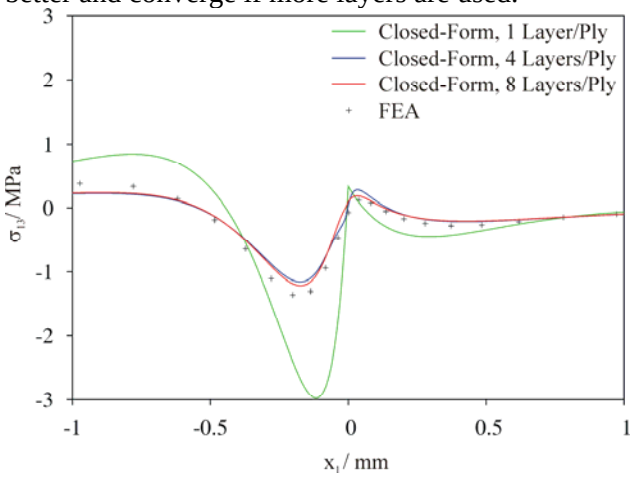

Fig. 5. Interlaminar shear stress σ_{13} in the range $-1\text{ mm} \le x_1 \le 1\text{ mm},\ x_2 = 2\text{ mm}$.

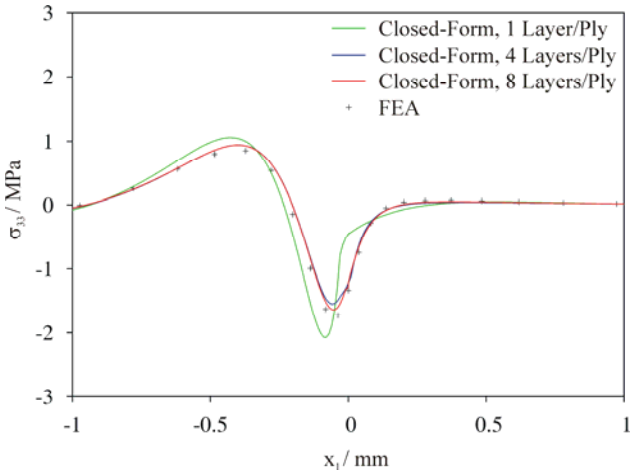

Fig. 6. Interlaminar normal stress σ_{33} in the range $-1\text{ mm} \le x_1 \le 1\text{ mm},\ x_2 = 2\text{ mm}$.

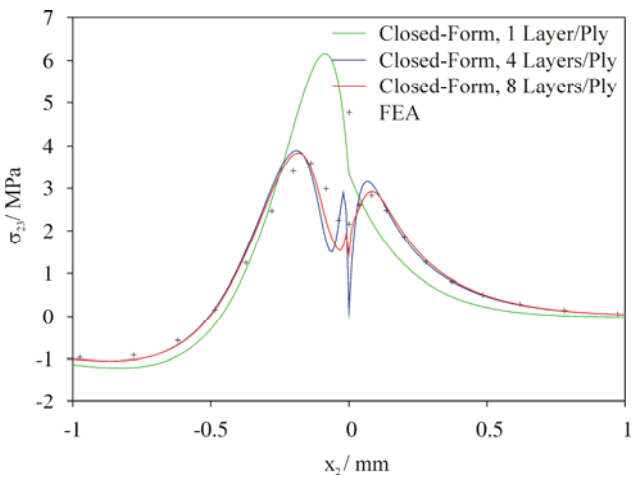

Fig. 7. Interlaminar shear stress σ_{23} in the range $-1\ \text{mm} \le x_2 \le\ 1\ \text{mm},\ x_1 = 2\ \text{mm}.$

In Fig. 6 and 8 the results for the interlaminar normal stress show the same trend as observed before.

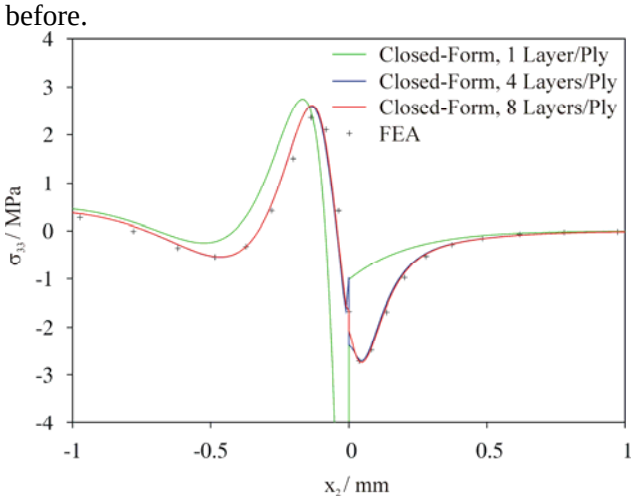

Fig. 8. Interlaminar normal stress σ_{33} in the range $-1\ \text{mm} \le x_2 \le\ 1\ \text{mm},\ x_1 = 2\ \text{mm}.$

3.3 Results of Interlaminar Stresses

As the foregoing results have shown a discretisation with eight layers per ply delivers well converged results. So, the subsequent analyses are performed with such a discretization. The analytical method is applied to obtain the stress field in the upper ply of the base laminate (second ply), the bottom ply of a reinforcement patch (third ply) and the fourth ply and again compared to numerical values of the accompanying FEA.

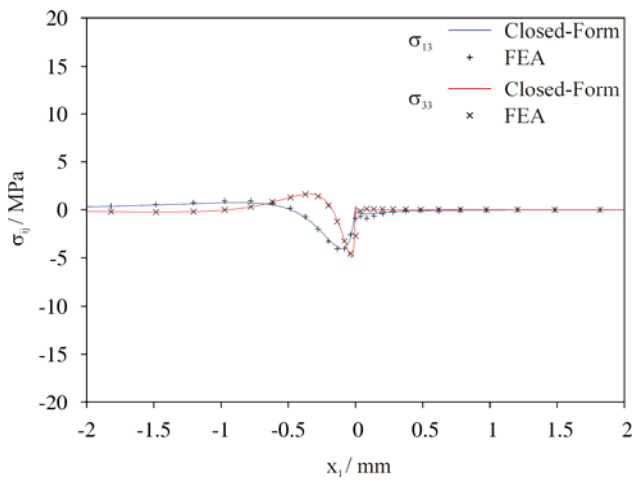

Fig. 9. Interlaminar stresses in the range $-2\ \text{mm} \le x_1 \le\ 2\ \text{mm},\ x_2 = 2\,\text{mm},\ x_3 = 0.48\,\text{mm}$

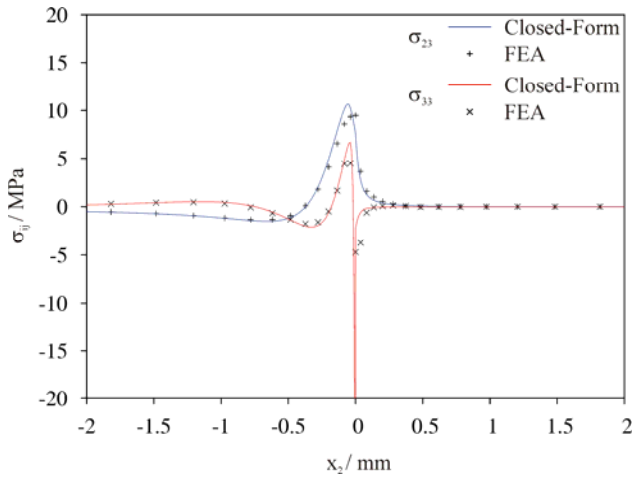

Fig. 10. Interlaminar stresses in the range $x_1 = 2\ \text{mm},\ 2\ \text{mm} \le x_2 \le\ 2\ \text{mm},\ x_3 = 0.48\,\text{mm}$

For the second ply it can be seen in Fig. 9 and 10 that the results agree very well with those from the FEA. Furthermore, the interlaminar normal stress at $x_3 = 0.48$ mm seems not critical since it assumes only low positive values close to $x_1 = 0$ mm and $x_2 = 0$ mm.

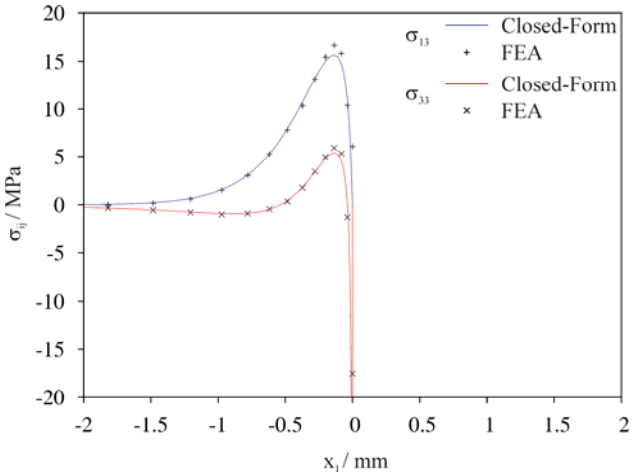

Fig. 11. Interlaminar stresses in the range $-2\ \text{mm} \le x_1 \le\ 2\ \text{mm},\ x_2 = 2\,\text{mm},\ x_3 = 0.73\,\text{mm}$

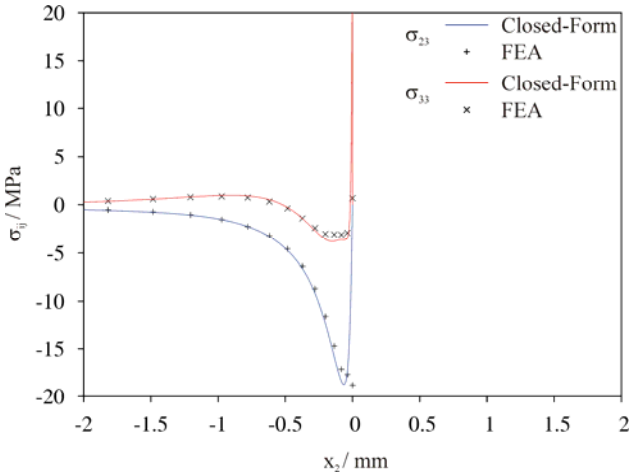

Fig. 12. Interlaminar stresses in the range $x_1 = 2\ \text{mm},\ -2\ \text{mm} \le x_2 \le\ 2\ \text{mm},\ x_3 = 0.73\,\text{mm}$

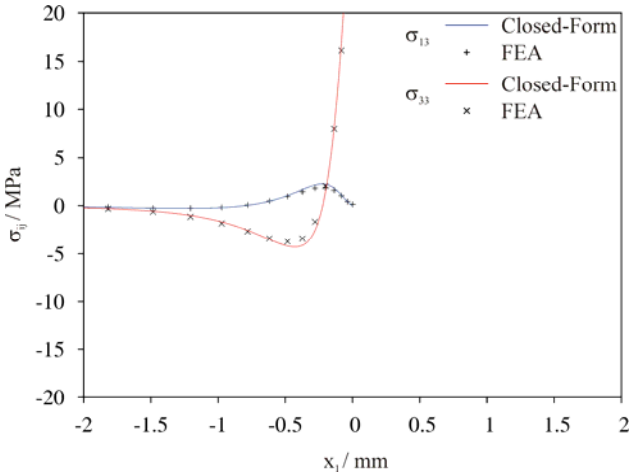

Fig. 13. Interlaminar stresses in the range $-2\ \text{mm} \le x_1 \le\ 2\ \text{mm},\ x_2 = 2\,\text{mm},\ x_3 = 0.98\,\text{mm}$

In the upper part of ply three at $x_3 = 0.73\,\text{mm}$ and the upper part of ply four at $x_3 = 0.98\,\text{mm}$ this is no longer true. There the interlaminar normal stresses tend to high positive values when close to $x_2 = 0\,\text{mm}$ and $x_1 = 0\,\text{mm}$, respectively, see Fig. 12 and 13. At the other free edges of the particular plies the interlaminar normal stress is due to its negative values no source of concern, see Fig. 11 and 14.

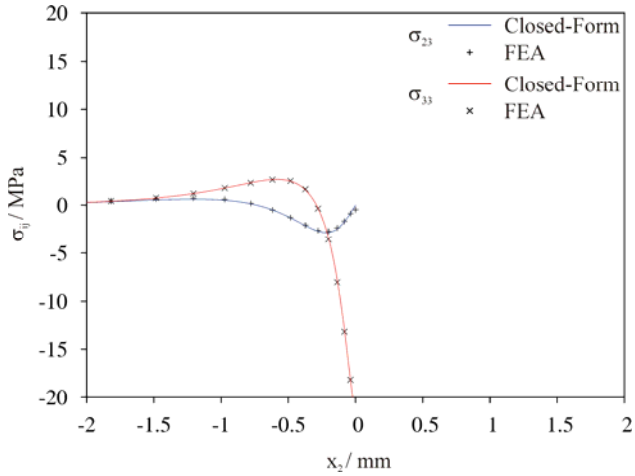

Fig. 14. Interlaminar stresses in the range $x_1 = 2\ \text{mm},\ -2\ \text{mm} \le x_2 \le\ 2\ \text{mm},\ x_3 = 0.98\,\text{mm}$

Subsequently, 3-D plots of the interlaminar normal stress situations in the three afore addressed plies at the respective x_3-coordinates $0.48\,\text{mm}$, $0.73\,\text{mm}$ and $0.98\,\text{mm}$ are shown in Fig. 15 to 17.

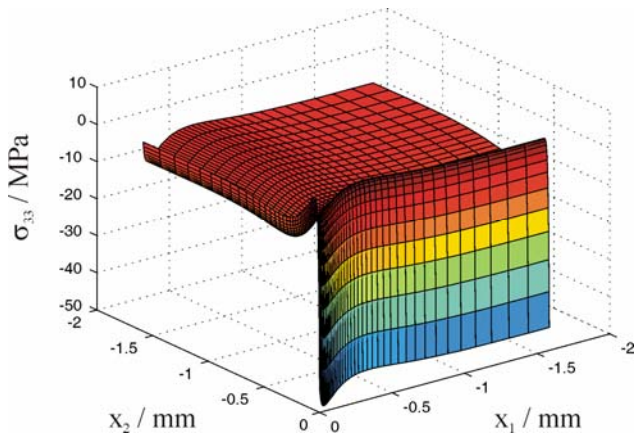

Fig. 15. Interlaminar normal stress in the second ply at $x_3 = 0.48\,\text{mm}$

The plots reveal that in plies 2 and 3 the interlaminar normal stress possesses a not very pronounced maximum close to the reinforcement patch corner. Contrary, the results for the interlaminar normal stress in ply 4 are not more severe towards the

corner than they are at one of the edges. This shows that knowing the stress field's behavior at a free edge is not sufficient to draw conclusions in regard to its behavior at the corner.

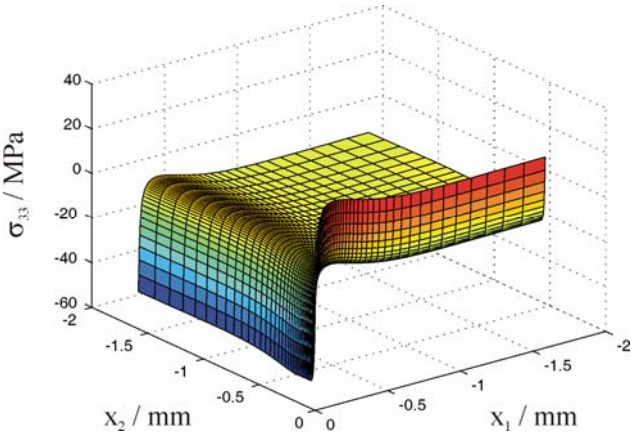

Fig. 16. Interlaminar normal stress in the third ply at $x_3 = 0.73\,\text{mm}$

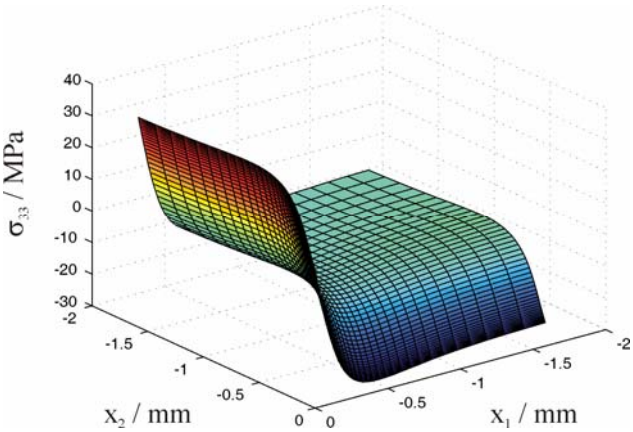

Fig. 17. Interlaminar normal stress in the fourth ply at $x_3 = 0.98\,\text{mm}$

4 Summary and Conclusion

For the stress field in the vicinity of a reinforcement patch corner of thermally loaded cross-ply laminates a closed-form three-dimensional approach has been presented. Basis for this procedure is the superposition of the in-plane stresses from the CLPT and a perturbing stress field. The perturbing stress field is developed with a layer-wise theory with unknown in-plane stress functions which are interpolated in the transversal direction. The in-plane stress functions are determined by the application of the principle of minimum complementary potential energy of the laminate which leads to a set of coupled ordinary differential equations. The boundary and transition conditions are fulfilled by employing an expanded Ritz-approach with Lagrange multipliers.

Studies in regard to the number of layers used by the closed-form approach show that convergence towards the results of accompanying finite-element calculations is achieved rapidly. This and the excellent agreement between the closed-form method and the finite element results give reliability to the method. The presented approach provides a valuable insight into the three-dimensional behavior of the stress field at a reinforcement patch corner. As the presented method is easily applicable and requires only a small percentage of the computational effort of a finite-element analysis it is particularly useful for more extensive parameter studies and optimization procedures.

References

[1] Reddy J.N. "*Mechanics of Laminated Composite Plates and Shells*". CRC Press, Boca Raton, 2004.

[2] Herakovich C.T. "Free Edge Effects in Laminated Composites". In Herakovich C.T. and Tarnopolskii Y.M. (eds.), Handbook of Composites, Structure and Design, Vol.2, pp.187-230, Elsevier Science Publishers B.V., Amsterdam, 1989.

[3] Kant T. and Swaminathan K. "Estimation of Transverse/Interlaminar Stresses in Laminated Composites, A Selective Review and Survey of Current Developments". *Composite Structures*, Vol. 4, pp 65-75, 2000.

[4] Mittelstedt C. and Becker W. "Interlaminar Stress Concentrations in Layered Structures Part I: A Selective Literature Survey on the Free-edge Effect Since 1967". *Journal of Composite Materials*, Vol. 38, pp 1037-1062, 2004.

[5] Becker W., Jin J.J. and Neuser P. "Interlaminar Stresses at the Free Corners of a Laminate". *Composite Structures*, Vol. 45, pp 155-162, 1999.

[6] Mittelstedt C. and Becker W. "Interlaminar Stress Concentrations in Layered Structures, Part II: Closed-form Analysis of Stresses at Laminated Rectangular Wedges with Arbitrary Non-orthotropic Layup" *Journal of Composite Materials*, Vol. 38, pp 1063-1090, 2004.

[7] Bhat N.V. and Lagace P.A."An Analytical Method for the Evaluation of Interlaminar Stresses Due to Material Discontinuities". *Journal of Composite Materials*, Vol. 28, pp 190–210, 1994.

[8] Wigger H.M. and Becker W. "Closed-Form Analysis of the Stress Field at Rectangular Corners of Reinforcement Patches". *Mechanics of Advanced Materials and Structures*, submitted.